Effect of the Pitch Modulation of Helical Coils on the Core Plasma Performance of the LHD-Type Helical Fusion Reactor*)

Takuya GOTO[1,2], Katsuji ICHIGUCHI[1,2], Hitoshi TAMURA[1,2], Junichi MIYAZAWA[1,2], Shinsuke SATAKE[1,2], Hiroyuki YAMAGUCHI[1,2], Nagato YANAGI[1,2] and the FFHR Design Group[1)]

[1)]*National Institute for Fusion Science, National Institutes of Natural Sciences, Toki, Gifu 509-5292 Japan*
[2)]*The Graduate University for Advanced Studies, SOKENDAI, Toki, Gifu 509-5292 Japan*

(Received 20 January 2021 / Accepted 13 May 2021)

The effect of the pitch modulation of the helical coils on the core plasma performance of the LHD-type helical fusion reactor has been examined. The analysis of the MHD stability and neoclassical transport for the pitch modulation $\alpha = 0.0$ and 0.1 has been conducted based on the finite-beta equilibrium calculated by the HINT code. It was found that the MHD stability is clearly improved without deteriorating the energy transport property by changing the pitch modulation α from 0.1 to 0.0. The reachable operation region expands to the higher density and the expected fusion gain can increase from ~10 to ~20. Because the change of the pitch modulation α from 0.1 to 0.0 requires only a slight change in the shape of the helical coils, the engineering design including the maintenance method that has been examined for the reactor with $\alpha = 0.1$ can be applied without a major modification.

Keywords: LHD-type helical reactor, pitch modulation, MHD stability, neoclassical transport, operation region

DOI: 10.1585/pfr.16.1405085

1. Introduction

Helical systems inherently have good features as a fusion power plant (capability of steady-state operation and high plant efficiency) and various concepts have been proposed by taking advantage of a high degree of freedom for the coil design. Among them, the heliotron system with two continuous helical coils has been leading the reactor design activity of the helical system for more than 20 years based on the quantity of the experimental data of the Large Helical Device (LHD), the experience in the construction and operation of the LHD, and the achievements of the engineering R&Ds in the National Institute for Fusion Science [1]. Recently, accuracy of the core plasma physics design of the LHD-type helical fusion reactor has been significantly improved by the combination of a new prediction method of the plasma parameters based on the direct extrapolation from the reference LHD experimental data and the validation of the predicted plasma parameters by utilizing the physics analysis tools developed for the analysis of the LHD experiment. Feasibility of the engineering design has also been improved through the three-dimensional design of the engineering components with consideration of the construction and the maintenance methods. Consequently, conceptual design of the LHD-type helical reactor FFHR-c1, which can demonstrate a year-long steady-state electric power generation with self-sufficient electricity and tritium fuel, has been proposed based on the core plasma performance confirmed by the LHD experiment [2].

On the other hand, a trade-off between good energy confinement and MHD stability has been recognized as one of the most important issues of the LHD-type heliotron system. If simultaneous achievement of good energy confinement and MHD stability at the higher level is realized, the requirement on the engineering design can be relaxed. This leads to the improvement of the attractiveness and the feasibility of the reactor design through the reduction of the construction cost and the developmental risk of the engineering components.

In the previous study, the effect of the pitch modulation of the helical coil α, which is one of the key parameters of the helical coil winding law, on the core plasma performance has been examined. The result indicated the possibility of simultaneous improvement of MHD stability and neoclassical transport by changing α from 0.1 (the same as that of the LHD) to 0.0 [2]. In that study, however, the analyses were conducted using the MHD equilibrium calculated by the 3D MHD equilibrium code VMEC [3] with the condition that the shape of the last closed flux surface (LCFS) is assumed to be the same as that in the vacuum equilibrium. Although this calculation method provides a fairly good estimation of the plasma property at the finite beta conditions, there is a concern regarding the reliability of the calculation results especially in the case of a high

author's e-mail: goto.takuya@nifs.ac.jp

*) This article is based on the invited talk at the 36th JSPF Annual Meeting (2019, Kasugai).

beta condition. On the other hand, it has been confirmed that the HINT code [4], which does not assume the existence of the nested magnetic surfaces, can reproduce the pressure profile and the Shafranov shift of the experimental results more accurately than the VMEC code. Because the calculation results of the MHD equilibrium and the neoclassical transport strongly depend on the MHD equilibrium, the calculation by the HINT code is important from the viewpoint of the improvement of the reliability and the cross-checking of the calculation result by the VMEC code.

Therefore, the effect of the pitch modulation on the core plasma performance of the LHD-type helical fusion reactor has been examined using the MHD equilibrium calculated by HINT code in this study. In the next section, a brief explanation of the helical coil winding law and the pitch modulation is given. Section 3 shows the calculation results regarding the effect of the pitch modulation on the MHD stability and the neoclassical transport. Section 4 shows the effect of the change in the pitch modulation on the operation region of the LHD-type helical fusion reactor.

2. Helical Coil Winding Law and Pitch Modulation

The trajectory of the guiding center of the helical coil of the heliotron device is described as follows:

$$R = R_c + a_c \cos\theta, \tag{1}$$

$$Z = a_c \sin\theta, \tag{2}$$

$$\theta = -\frac{m}{\ell}\phi - \alpha \sin\left(\frac{m}{\ell}\phi\right), \tag{3}$$

where R_c, a_c, θ, ϕ, m, ℓ and α are helical coil major radius, helical coil minor radius, poloidal angle, toroidal angle, toroidal pitch number, poloidal pitch number (the number of helical coils) and pitch modulation, respectively. In place of the helical coil minor radius, helical pitch parameter

$$\gamma_c = \frac{m a_c}{\ell R_c}, \tag{4}$$

is often used both in the physics analysis and in the engineering design. In the past, heliotron devices with various sets of these coil design parameters have been designed and constructed [5–8]. In the conceptual design study of the LHD-type helical reactor FFHR, the same set of the coil design parameters as that of the LHD has been selected: $m = 10$, $\ell = 2$ and $\alpha = 0.1$. Regarding the helical pitch parameter, the geometric shape of the helical coils of the LHD corresponds to $\gamma_c = 1.25$. However, the helical coil of the LHD consists of three blocks and the current center of the helical coil can be varied by changing the ratio of the current of each block. In the design study of FFHR-d1, $\gamma_c = 1.2$ has been selected because the magnetic surface structure which is similar to that in the vacuum equilibrium can be achieved with a high beta condition ($\beta_0 \sim 8\%$) in this configuration by applying adequate vertical field [9]. The change in the pitch number m and the number of helical coils ℓ requires a fundamental revision of the engineering design. Therefore, in this study the pitch modulation α was selected as a key parameter and the other parameters were set to be the same as those of FFHR-d1: $m = 10$, $\ell = 2$ and $\gamma_c = 1.2$. Figure 1 shows the trajectory of the guiding center of one helical coil with pitch modulations on the plane of the toroidal angle and the poloidal angle. Figure 2 shows the comparison of the shape of the helical coil for $\alpha = 0.1$ and 0.0. The change of the helical coil shape by the change of α from 0.1 to 0.0

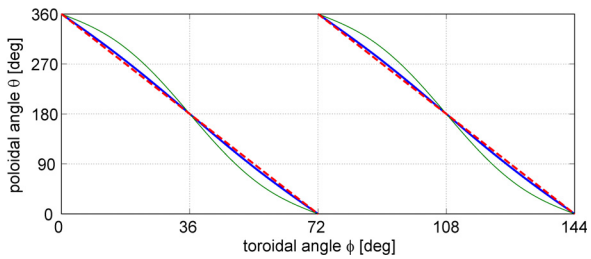

Fig. 1 Comparison of the trajectory of the guiding center of the helical coil. The thick solid blue line and the thick dotted red line correspond to $\alpha = 0.1$ and 0.0, respectively. The thin green line is a reference of $\alpha = 0.5$.

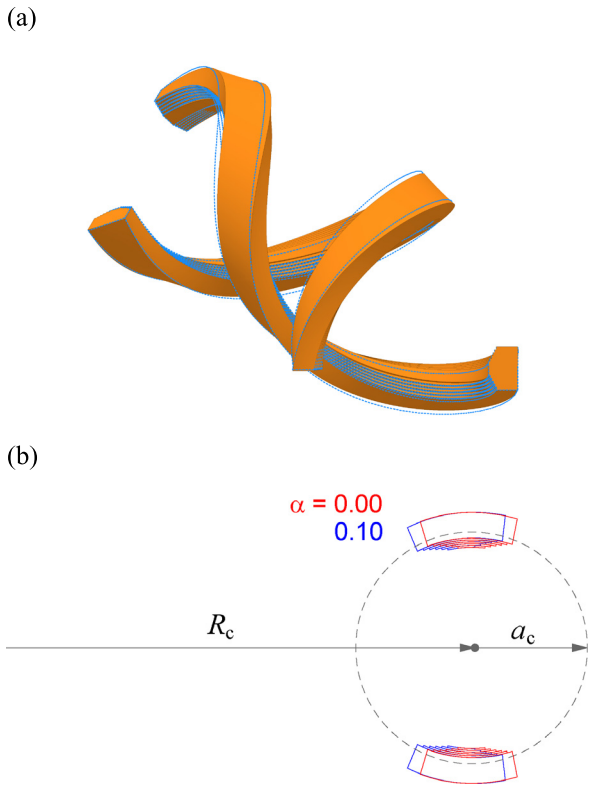

Fig. 2 (a) Comparison of the 3D shape of helical coil for $\alpha = 0.0$ (solid object) and 0.1 (broken lines). (b) Comparison of the poloidal cross-section of the helical coil for $\alpha = 0.0$ (red) and 0.1 (blue).

is quite small.

The effect of α on the plasma performance was already investigated in the design activity of the LHD. Although it was expected that both the MHD stability and the particle confinement improve with decreasing α, $\alpha = 0.1$ was finally selected to ensure the effective divertor configuration. In the case of a reactor with a larger size, the area of the helical coil becomes relatively small. In addition, several methods to increase the space between the helical coil and the plasma has been proposed, for example, the change of the cross-sectional shape of the coil and the placement of supplementary helical coils [10]. The physics analysis tools have also been significantly improved from the days of the LHD design phase. Therefore, the close investigation of the plasma performance for $\alpha = 0.0$ is important from the viewpoint of the reactor design. Regarding the effect of the pitch modulation α, another approach of the configuration optimization by the simultaneous change of the pitch modulation and the ratio of helical coil minor radius in the vertical direction to that in the horizontal direction has also been proposed from the viewpoint of the vacuum field structure [11]. In this study, we focused on the analysis of $\alpha = 0.0$ because it is important to extract the effect of the change in the pitch modulation.

3. Effect of the Pitch Modulation on Core Plasma Performance

In this study, examination of the effect of the pitch modulation on the core plasma performance was conducted by the following 3 methods.

- 3D MHD equilibrium analysis by HINT [4]
- linear MHD stability analysis by KSPDIAG [12]
- neoclassical transport analysis by GSRAKE [13]

In the MHD equilibrium analysis, the calculation result can be applied to the device of a similar shape by similarity expansion if the beta value is the same. Because there are several design options with a different size for the FFHR, the reference data with the size of the LHD ($R_c = 3.9$ m)

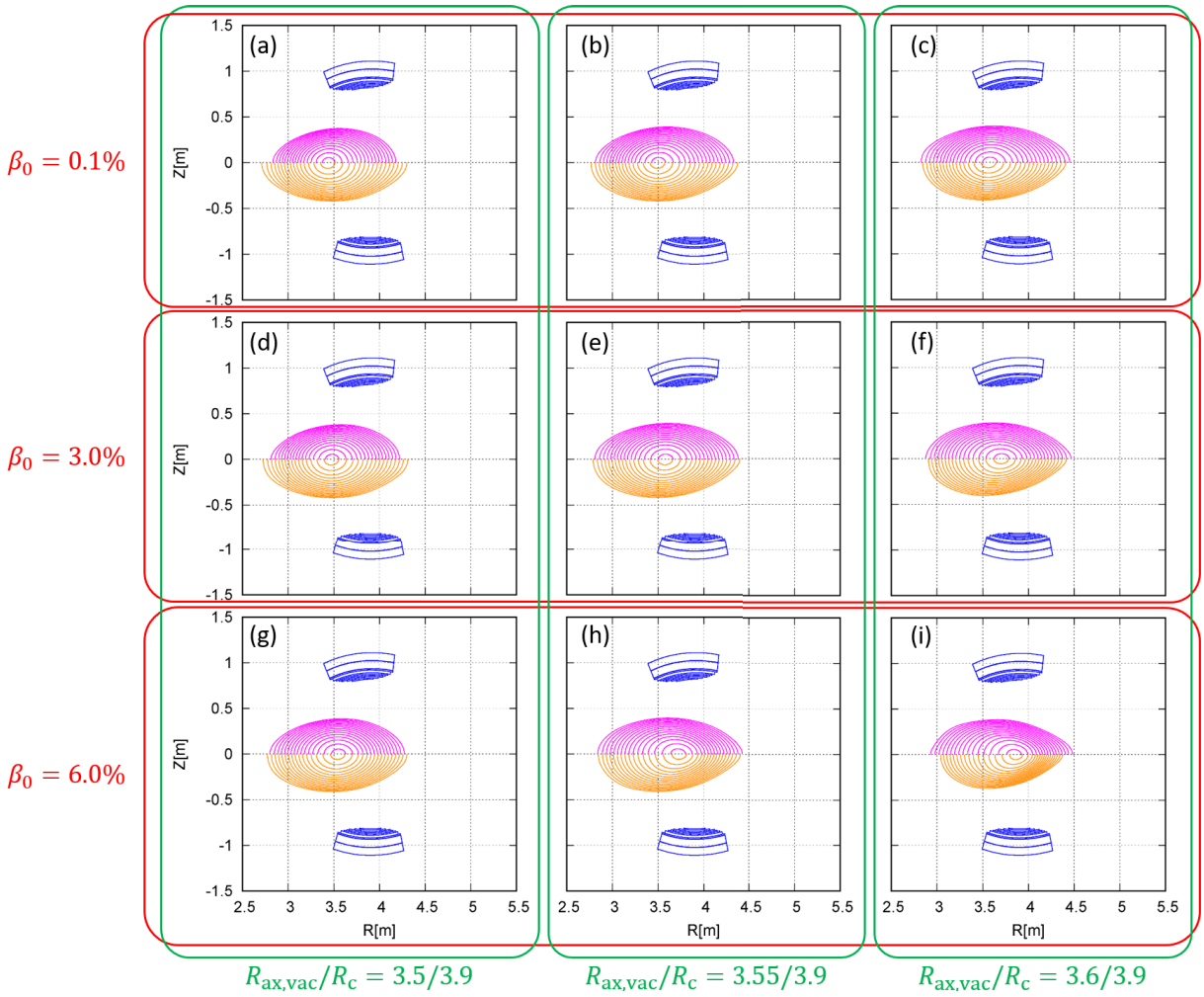

Fig. 3 The magnetic surface shape at horizontally-elongated poloidal cross-section calculated by the HINT code with different beta values and magnetic axis positions at the vacuum equilibrium for the reference device with $R_c = 3.9$ m. The upper side (magenta color) and the lower side (orange color) of each plot correspond to $\alpha = 0.1$ and 0.0, respectively. The shape of the helical coils is also plotted.

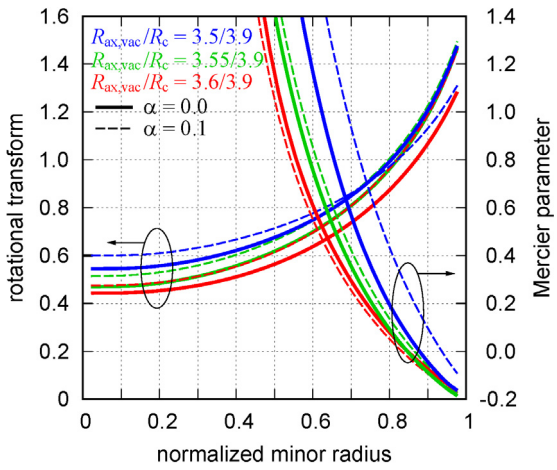

Fig. 4 Comparison of the radial profiles of rotational transform and the Mercier parameter D_I at the peak beta of β_0 = 3.0%. Thick solid lines and thin broken lines correspond to α = 0.1 and 0.0, respectively. The line color of red, green, and blue correspond to the magnetic axis position at the vacuum equilibrium of $R_{ax,vac}/R_c$ = 3.5/3.9, 3.55/3.9, and 3.6/3.9, respectively.

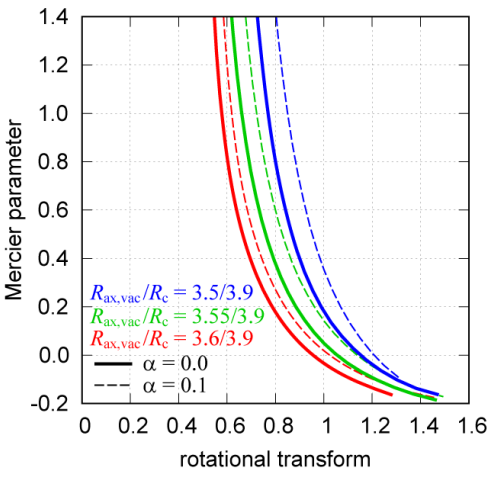

Fig. 5 Comparison of the profiles of the Mercier parameter as a function of the rotational transform at the beak beta of β_0 = 3.0%. Thick solid lines and thin broken lines correspond to α = 0.1 and 0.0, respectively. The values at the horizontal axis of 1 correspond to that of D_I at m/n = 1/1 rational surface. The meaning of the line type and color is identical to those of Fig. 4.

has been prepared by the HINT code. In the calculations of KSPDIAG and GSRAKE, the MHD equilibrium calculated by the VMEC with the shape of the LCFS that is scaled from the reference data obtained by the HINT calculation was used.

Figure 3 shows the comparison of magnetic surface shapes of α = 0.1 and 0.0 of the reference device (R_c = 3.9 m) at horizontally-elongated poloidal cross-section with different magnetic axis positions at the vacuum equilibrium $R_{ax,vac}$ (corresponds to the difference in the currents of the vertical field coils) for the peak beta of β_0 = 0.1%, 3.0% and 6.0%, respectively. The results show that the shift of magnetic axis position by the increase of the beta value does not depend so much on α. On the other hand, the volume enclosed by the LCFS strongly depends on α and the magnetic axis position. The magnetic axis position that gives the maximum volume for α = 0.0 is to be further inward than that for α = 0.1.

Figure 4 shows the radial profile of the rotational transform and the Mercier parameter D_I [14] for different magnetic axis positions and pitch modulations. It was found that the rotational transform in the core region of α = 0.0 is smaller than that of α = 0.1 for any magnetic axis position. The Mercier parameter D_I of α = 0.0 is smaller than that of α = 0.1 in the entire plasma region for any magnetic axis position. Figure 5 shows the relation between the rotational transform and the Mercier parameter. In the LHD experiment, it has been observed that a low-n MHD mode becomes unstable and causes the collapse of the core pressure when D_I at m/n = 1/1 rational surface (corresponding to the radial position with $\iota/2\pi$ = 1) exceeds 0.2 - 0.3. Because D_I at the radial position of $\iota/2\pi$ = 1 for α = 0.0 is smaller than that of α = 0.1,

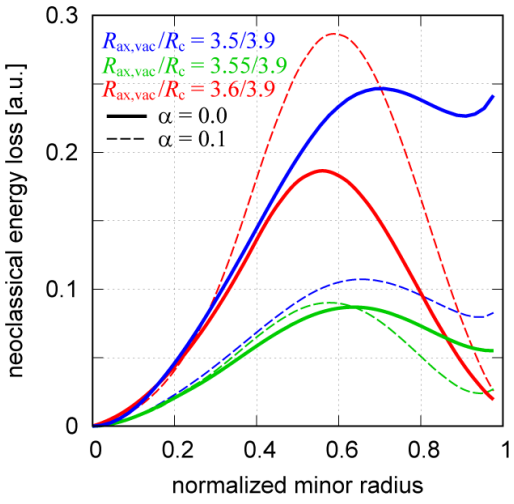

Fig. 6 Comparison of the radial profile of the neoclassical energy loss at the peak beta of β_0 = 3.0%. The meaning of the line type and color is identical to those of Fig. 4.

it can be concluded that α = 0.0 is better than α = 0.1 from the viewpoint of the MHD stability. In the case of $R_{ax,vac}/R_c \geq$ 3.55/3.9, m/n = 2/1 rational surface emerges around the core region. Because the rotational transform in the core region decreases with increasing the beta value, this m/n = 2/1 rational surface can emerge in the case of $R_{ax,vac}/R_c \leq$ 3.55/3.9. Although there is no clear criterion for the MHD stability at m/n = 2/1 rational surface, this effect of the decreasing in the core rotational transform should be carefully investigated. On the other hand, the rotational transform can be controlled by a method other than the change in the magnetic axis position, for example, control of the quadrupole field components. There-

fore, $\alpha = 0.0$ is considered to be better than 0.1 from the viewpoint of MHD stability.

Figure 6 shows the radial profile of neoclassical energy loss. The results indicate that there is an optimum magnetic axis position that minimizes the neoclassical transport and the optimum position is different between $\alpha = 0.0$ and 0.1. It is expected that the optimum magnetic axis position for $\alpha = 0.0$ is to be more outward than that of $\alpha = 0.1$, which is preferable from the viewpoint of the suppression of the MHD stability.

4. Effect of the Pitch Modulation on the Operation Region of the LHD-Type Helical Fusion Reactor

To investigate the impact of the change in the pitch modulation on the operation region of the LHD-type helical fusion reactor, parametric scans of the electron density and the electron temperature have been conducted for FFHR-c1 with $R_c = 10.92$ m and $B_c = 7.3$ T. In this analysis, the same radial profile of the electron density as that in the previous study is assumed. The radial profile of the ion density is assumed to be the same as that of the electron density. The radial profiles of the electron temperature and the ion temperature are calculated from those of the electron pressure and ion pressure, which are given as

$$p_e(\rho) = \gamma_{\mathrm{DPE}*}\hat{p}(\rho)P_{\mathrm{abs,e}}^{0.4}B^{0.8}n_e(\rho)^{0.6}, \quad (5)$$

$$p_i(\rho) = \gamma_{\mathrm{DPE}*}\hat{p}(\rho)P_{\mathrm{abs,i}}^{0.4}B^{0.8}n_i(\rho)^{0.6}, \quad (6)$$

where B, n_e and n_i are the magnetic field strength, the electron density and the ion density, respectively. The terms of the total absorbed power in Eqs. (5) and (6) are given as

$$P_{\mathrm{abs,e}} = \eta_\alpha P_\alpha + \eta_{\mathrm{aux}}P_{\mathrm{aux}} - P_{\mathrm{rad}} - P_{\mathrm{ei}}, \quad (7)$$

$$P_{\mathrm{abs,i}} = P_{\mathrm{ei}}, \quad (8)$$

where η_α, P_α, η_{aux}, P_{aux}, P_{rad}, and P_{ei} are the absorbed efficiency of alpha heating, the alpha power, the absorbed efficiency of auxiliary heating, the auxiliary heating power, the power loss by radiation and the equipartition power from electrons to ions, respectively. $\hat{p}(\rho)$ in Eqs. (5) and (6) is the gyro-Bohm normalized pressure of the reference LHD experimental data

$$\hat{p}(\rho) = \frac{p_{\mathrm{e,exp}}(\rho)}{P_{\mathrm{abs,exp}}^{0.4}B_{\mathrm{exp}}^{0.8}n_{\mathrm{e,exp}}(\rho)^{0.6}}, \quad (9)$$

where the subscript 'exp' denotes that the parameters are obtained from the reference LHD experimental data. $\gamma_{\mathrm{DPE}*}$ in Eqs. (5) and (6) are the confinement improvement factor related to the peakedness of the heating profile [15]. The definition is given by

$$\gamma_{\mathrm{DPE}*} = \left\{\frac{(P_{\mathrm{dep}}/P_{\mathrm{dep1}})_{\mathrm{avg}}}{(P_{\mathrm{dep}}/P_{\mathrm{dep1}})_{\mathrm{avg,exp}}}\right\}^{0.6}, \quad (10)$$

$$(P_{\mathrm{dep}}/P_{\mathrm{dep1}})_{\mathrm{avg}} = \int_0^1 \frac{P_{\mathrm{dep}}(\rho)}{P_{\mathrm{dep}}(1)}\mathrm{d}\rho, \quad (11)$$

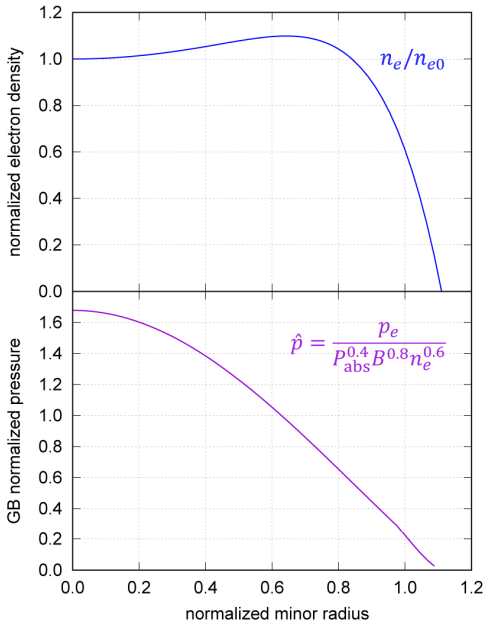

Fig. 7 Radial profiles of (upper) normalized electron density and (lower) gyro-Bohm normalized pressure used in this study.

$$P_{\mathrm{dep}}(\rho) = \int_0^\rho P_{\mathrm{abs}}(\rho')\left(\frac{\mathrm{d}V}{\mathrm{d}\rho'}\right)\mathrm{d}\rho'. \quad (12)$$

The radial profile of the normalized electron density and the gyro-Bohm normalized pressure used in this study are shown in Fig. 7.

Figure 8 shows the plasma operation contour (POPCON) plot for the pitch modulations of $\alpha = 0.1$ and 0.0. In the calculation for $\alpha = 0.1$, the MHD equilibrium which is the same as that in the previous study [2] was used. In the calculation for $\alpha = 0.0$, the MHD equilibrium with $R_{\mathrm{ax,vac}}/R_c = 3.55/3.9$ and $\beta_0 = 3.0\%$ (shown in Fig. 3) was used. The contours of Mercier parameter D_I at $m/n = 1/1$ rational surface, the ratio of the neoclassical transport loss to the accumulative volume integral of the absorbed power (the maximum value in the radial profile) $(Q_{\mathrm{neo}}S/P_{\mathrm{abs}})_{\mathrm{max}}$ and the fusion gain Q are plotted. In the LHD experiment, it has been observed that D_I at $m/n = 1/1$ rational surface is limited up to 0.2 - 0.3. It has also been observed that a certain ratio of the energy loss is caused by the anomalous transport, hence $(Q_{\mathrm{neo}}S/P_{\mathrm{abs}})_{\mathrm{max}} < 1$. In Fig. 8, the region that does not satisfy these conditions is shaded. Comparing the region without shading, it was found that the reachable operation region extends to the higher density in the case of $\alpha = 0.0$ because of the decrease in D_I at the same density or beta value. Consequently, the achievable fusion gain can increase from ~10 to ~20 by changing α from 0.1 to 0.0. The increase of the fusion gain by changing α can also be confirmed by the calculation using the VMEC code. However, the estimated neoclassical energy loss at the same electron density and temperature is larger because the shift of the

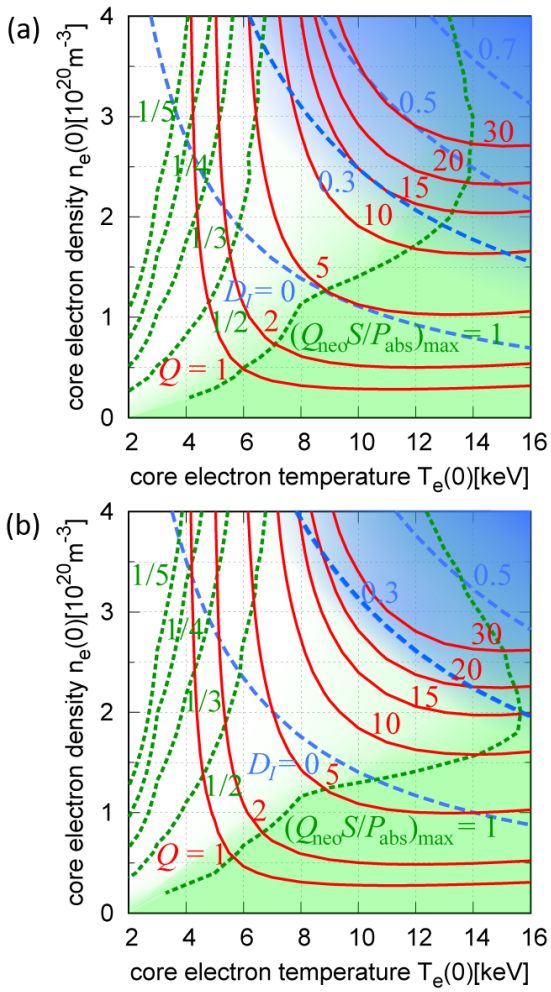

Fig. 8 POPCON plot of (a) $\alpha = 0.1$ and (b) $\alpha = 0.0$. Contours of the Mercier parameter (broken blue curve), the ratio of the neoclassical energy loss to the total absorbed power (dotted green curve) and the fusion gain (red solid curve) are plotted. The area without shading corresponds to the reachable operation region with the physics conditions confirmed by the LHD experiment.

magnetic axis position is overestimated. The estimated fusion power at the same electron density and temperature is smaller because the plasma volume is underestimated. These factors cause the shift of the operation limit due to the neoclassical energy loss to the lower temperature side and the shift of the contours of the fusion gain to the higher density and temperature side, resulting in an underestimation of the fusion gain by a factor of ~0.7. Consequently, the calculation by the HINT code is important for accurate evaluation of the reachable operation region and the fusion gain.

5. Summary

The effect of the pitch modulation of the helical coil on the core plasma performance of the LHD-type helical fusion reactor has been examined. It was confirmed that the Mercier parameter, which is an index for the MHD stability, is clearly improved without deteriorating the energy transport property by changing the pitch modulation α from 0.1 to 0.0. This improvement expands the reachable operation region to higher density and the achievable fusion gain of FFHR-c1 can increase from ~10 to ~20.

Although further detailed physics analysis including the fast particle confinement and bootstrap current is required, it was confirmed that the plasma performance of the LHD-type helical reactor can be improved by a slight change in the winding law of the helical coils. There is room for further improvement of the plasma performance by optimizing the winding law. This means the plasma performance of the LHD-type helical fusion reactor can be significantly improved without major impact on the engineering design including a maintenance method that has been established in the past study. It is expected that the design feasibility and the attractiveness of the LHD-type helical fusion reactor will be enhanced by such optimization of the helical coil winding law.

This work is supported by the budget NIFS11UFFF011 of National Institute for Fusion Science. The authors thank Dr. Yasuhiro Suzuki for his permission to use the HINT code. The authors also appreciate the members of the Fusion Engineering Research Project in NIFS for providing valuable comments and advice.

[1] A. Sagara *et al.*, Nucl. Fusion **57**, 086046 (2017).
[2] T. Goto *et al.*, Nucl. Fusion **59**, 076030 (2019).
[3] S.P. Hirshman *et al.*, Phys. Fluids **26**, 3553 (1983).
[4] Y. Suzuki *et al.*, Nucl. Fusion **46**, L19 (2006).
[5] K. Uo *et al.*, Plasma Physics and Controlled Nuclear Fusion Research (Proc. 11th Int. Conf. Kyoto, 1986), Vol. 2, IAEA, Vienna 355 (1987).
[6] K. Nishimura *et al.*, Fusion Technol. **17**, 86 (1990).
[7] A. Iiyoshi *et al.*, Nucl. Fusion **39**, 1245 (1999).
[8] T. Obiki *et al.*, Nucl. Fusion **41**, 803 (2001).
[9] J. Miyazawa *et al.*, Nucl. Fusion **54**, 043010 (2014).
[10] N. Yanagi *et al.*, Plasma Fusion Res. **11**, 2405034 (2016).
[11] N. Yanagi *et al.*, J. Fusion Energy **38**, 147 (2019).
[12] Y. Nakamura *et al.*, J. Phys. Soc. Jpn. **58**, 3157 (1989).
[13] C.D. Beidler *et al.*, Plasma Phys. Control. Fusion **37**, 463 (1995).
[14] A.H. Glasser *et al.*, Phys. Fluids **18**, 875 (1975).
[15] J. Miyazawa *et al.*, Nucl. Fusion **54**, 013014 (2014).